Physiological levels of TNFα stimulation induce stochastic dynamics of NF-κB responses in single living cells

David A. Turner[1], Pawel Paszek[1], Dan J. Woodcock[2], David E. Nelson[1], Caroline A. Horton[1], Yunjiao Wang[3], David G. Spiller[1], David A. Rand[2], Michael R. H. White[1,*] and Claire V. Harper[1]

[1]Centre for Cell Imaging, School of Biological Sciences, Bioscience Research Building, Crown Street, Liverpool, L69 7ZB, UK
[2]Warwick Systems Biology, Coventry House, University of Warwick, Coventry, CV4 7AL, UK
[3]School of Mathematics, University of Manchester, M13 9PL UK and Manchester Interdisciplinary Biocentre, University of Manchester, M1 7DN, UK

*Author for correspondence (m.white@liv.ac.uk)

Accepted 26 May 2010
Journal of Cell Science 123, 2834-2843

doi:10.1242/jcs.069641

Summary

Nuclear factor kappa B (NF-κB) signalling is activated by cellular stress and inflammation and regulates cytokine expression. We applied single-cell imaging to investigate dynamic responses to different doses of tumour necrosis factor alpha (TNFα). Lower doses activated fewer cells and those responding showed an increasingly variable delay in the initial NF-κB nuclear translocation and associated IκBα degradation. Robust 100 minute nuclear:cytoplasmic NF-κB oscillations were observed over a wide range of TNFα concentrations. The result is supported by computational analyses, which identified a limit cycle in the system with a stable 100 minute period over a range of stimuli, and indicated no co-operativity in the pathway activation. These results suggest that a stochastic threshold controls functional all-or-nothing responses in individual cells. Deterministic and stochastic models simulated the experimentally observed activation threshold and gave rise to new predictions about the structure of the system and open the way for better mechanistic understanding of physiological TNFα activation of inflammatory responses in cells and tissues.

Key words: NF-κB, TNFα, Live-cell imaging, Stochastic processes, Mathematical modelling, Systems biology

Introduction

Nuclear factor kappaB (NF-κB) describes a family of dimeric transcription factors, comprising the ubiquitously expressed RelA–p50 heterodimer. NF-κB regulates the expression of more than 300 genes involved in processes such as inflammation, immunity and cell survival (Aggarwal, 2000; Hayden and Ghosh, 2008). NF-κB dimers are sequestered in the cytoplasm through association with members of the inhibitor kappaB (IκB) family, preventing their nuclear accumulation. Stimulation by inflammatory mediators such as tumour necrosis factor alpha (TNFα) causes the activation of the IκB kinase (IKK) complex, which targets NF-κB-bound IκB proteins for phosphorylation, leading to their ubiquitin-mediated proteasomal degradation (Zandi et al., 1998). The liberated NF-κB translocates to the nucleus, where it regulates the expression of a plethora of target genes such as cytokines, chemokines and NF-κB and IκB family members that are involved in negative feedback. In the presence of sustained TNFα stimulation, NF-κB translocates into and out of the nucleus with a period of approximately 100 minutes, and is dependent on the continual degradation and re-synthesis of IκB proteins (Ashall et al., 2009; Friedrichsen et al., 2006; Nelson et al., 2004). These oscillations are important in temporal regulation of gene transcription, because varying the frequency of NF-κB translocations can produce distinct gene expression profiles (Ashall et al., 2009). The concept of frequency encoding of biological output functions originated from studies of Ca^{2+} oscillations, where the strength of the response is encoded by the amplitude and frequency of changes in intracellular Ca^{2+} concentration (Berridge et al., 1998; Dolmetsch et al., 1997; Dolmetsch et al., 1998).

Cells stimulated with TNFα have the ability to secrete various cytokines, including TNFα itself. This could result in positive feedback that in turn might affect NF-κB signalling (Coward et al., 2002; Lee et al., 2009). The strength of this positive feedback is crucial to regulate the balance between propagation of the inflammatory response and its eventual resolution. Failure to regulate this balance is often indicative of many autoimmune diseases such as chronic sepsis and arthritis. A number of studies have reported that the physiological levels of TNFα in human plasma (Nakai et al., 1999), mouse tissues (Matalka et al., 2005) and in the serum of patients surviving acute sepsis (Damas et al., 1989) are much lower than those levels used to elicit maximum responses in many experimental studies (10 ng/ml). Serum TNFα concentrations up to 5 ng/ml were found in patients who did not survive acute sepsis (Damas et al., 1989), indicating a disparity between physiological and pathogenic TNFα levels. The type 1 TNFα receptor (TNF-R1) has a very high affinity for soluble TNFα (Grell et al., 1998), suggesting that the system might detect and respond to low concentrations of TNFα. System sensitivity for low TNFα concentrations is potentially increased through interaction with TNF-R2 receptors that have the ability to effectively increase local TNFα concentration (Butera et al., 1996; Tartaglia et al., 1993). Indeed, some cell lines have been shown to be sensitive to TNFα levels as low as 8 pg/ml (Khabar et al., 1995).

One key characteristic of the response to 10 ng/ml TNFα is that individual cells show oscillations in NF-κB cellular localisation that are out of phase between cells (Ashall et al., 2009; Nelson et al., 2004). This means that these oscillations cannot be observed at the

population level. Therefore, when probing the response to stimulation with lower doses of TNFα, it is important to consider not only the average population response, but also the possible heterogeneity between cells that would otherwise be missed. A population-level analysis suggested that at low TNFα doses, cells produce damped responses that are homogenous across the population (Cheong et al., 2006). By contrast, a theoretical study by Lipniacki and colleagues suggested that system activation at low doses might be very stochastic; however, a full NF-κB response might be achieved even at the picomolar TNFα concentration (proposed to be due to the binding of a single TNFα trimer) (Lipniacki et al., 2007). This theoretical analysis predicted the existence of a threshold for system activation associated with an event within a TNF-R1–IKK transduction pathway.

We have investigated the contribution of single-cell dynamics to the overall population responses to TNFα and show that the heterogeneity between cells is increased at low doses of TNFα. A combination of live-cell imaging and mathematical modelling was used to assess the NF-κB nuclear translocation kinetics in single living SK-N-AS cells following stimulation with a range of TNFα doses (1 pg/ml to 10 ng/ml). These data show that cells could still display robust 100 minute oscillations, but as the TNFα dose was lowered, the fraction of cells responding decreased and the cells showed a stochastic delay in their response. These data support the concept of a threshold for system activation, which might arise from variable inhibitor expression or from noisy upstream processes in the TNFα pathway. Deterministic and stochastic models simulated this activation threshold and allowed a better mechanistic understanding of physiological TNFα activation of inflammatory responses in cells and tissues.

Results

Dose-dependent activation of reporter gene expression by TNFα

Previous reports have shown that cells have the ability to respond to a wide range of TNFα doses (Cheong et al., 2006; Khabar et al., 1995). Therefore, we investigated the sensitivity of human SK-N-AS neuroblastoma cells to a wide range of TNFα concentrations using a luciferase reporter assay.

SK-N-AS cells were transfected with either a consensus (NF-Luc) or a specific (IκBα-Luc) NF-κB-inducible luciferase reporter gene. We observed a dose-dependent upregulation of expression of both reporter genes, with a maximal response at 10 ng/ml TNFα (Fig. 1A,B). Following stimulation with doses above 10 pg/ml, there was a significant increase ($P \leq 0.05$) in signal from the NF-Luc reporter construct at 4 hours compared with untreated cells (Fig. 1A). However, following stimulation with 10 pg/ml TNFα, no significant increase in signal was detectable until 6 hours after treatment (Fig. 1A). A similar response pattern was observed with the IκBα-Luc reporter gene construct (Fig. 1B). This shows that, as previously observed in studies of other cell types (e.g. Cheong et al., 2006; Khabar et al., 1995), TNFα elicits a dose-dependent rise in NF-κB activation.

RelA-dsRedxp translocation dynamics are dose dependent

Cell population analysis, using techniques such as EMSA (electrophoretic mobility shift assay), western blotting and RT-PCR, are informative on average responses, but mask the cellular heterogeneity inherent in the NF-κB system (Ashall et al., 2009; Nelson et al., 2004). It is therefore not possible to discern whether

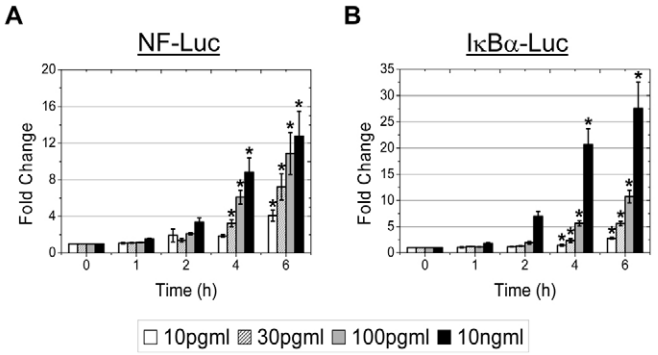

Fig. 1. Dose- and time-dependent activation of NF-κB-inducible gene expression by TNFα. SK-N-AS cells were transiently transfected with the NF-Luc (**A**) or IκBα-Luc (**B**) reporter constructs and were stimulated with either 10 pg/ml, 30 pg/ml, 100 pg/ml or 10 ng/ml TNFα for up to 6 hours. The luminescence signal was measured at five time points and the fold change in luminescence relative to control values was calculated. Error bars ± s.e.m. from three replicate experiments. *$P \leq 0.05$ by ANOVA.

the reductions in signal amplitude from population assays (Fig. 1A,B) are due to a homogenous reduction in the amplitude of the response in all cells, or to heterogeneous responses from a subset of cells. Therefore, the dose-dependent response of single cells to TNFα was measured by observing the dynamics of the first nuclear translocation of fluorescently tagged RelA (RelA-dsRedxp) (Fig. 2).

Stimulation with high doses of TNFα (100 pg/ml and above) showed relatively synchronous initial nuclear translocations and gave comparatively large N:C amplitudes with a great degree of heterogeneity (Fig. 2). An intermediate dose of TNFα (30 pg/ml) reduced the synchrony in the time to the initial nuclear translocation with some translocations being highly delayed and gave a significant reduction ($P \leq 0.05$) in the N:C amplitude (Fig. 2). At doses <30 pg/ml, a random delay in timing of the initial response was observed with many cells showing significantly delayed responses ($P \leq 0.05$) compared with cells treated with higher doses of TNFα (Fig. 2A,B). The timing of the first translocation induced by different doses of TNFα was not correlated with the intensity (protein concentration) of RelA-dsRedxp or the control EGFP (supplementary material Fig. S1, Fig. S2A-E). There was no difference in the N:C amplitude between doses of TNFα below 30 pg/ml TNFα and mock stimulation (Fig. 2C). The initial response times in cells exposed to TNFα (0, 1, 3 and 30 pg/ml) were not significantly different as a result of the very high degree of variability with no TNFα addition, only doses ≥100 pg/ml differed significantly from the control (Fig. 2B).

The dose of stimulus also affected the percentage of cells showing detectable TNFα-induced RelA-dsRedxp translocations (Fig. 2D). Stimulation with vehicle alone (medium) resulted in ~18% of cells showing an apparently significant translocation event (response) within a 300 minute period of measurement (Fig. 2D; see supplementary material Table S1A; see Materials and Methods for definition of a response). However, as the concentration of TNFα was increased, a significant rise ($P \leq 0.05$) in the number of cells responding was observed above a concentration of 1 pg/ml. At doses of 100 pg/ml and greater, 100% of cells analysed responded (Fig. 2D). Although ~28% of cells responded at 1 pg/ml compared with ~18% in the control (see supplementary material Table S1A), this was not statistically significant (Fig. 2D).

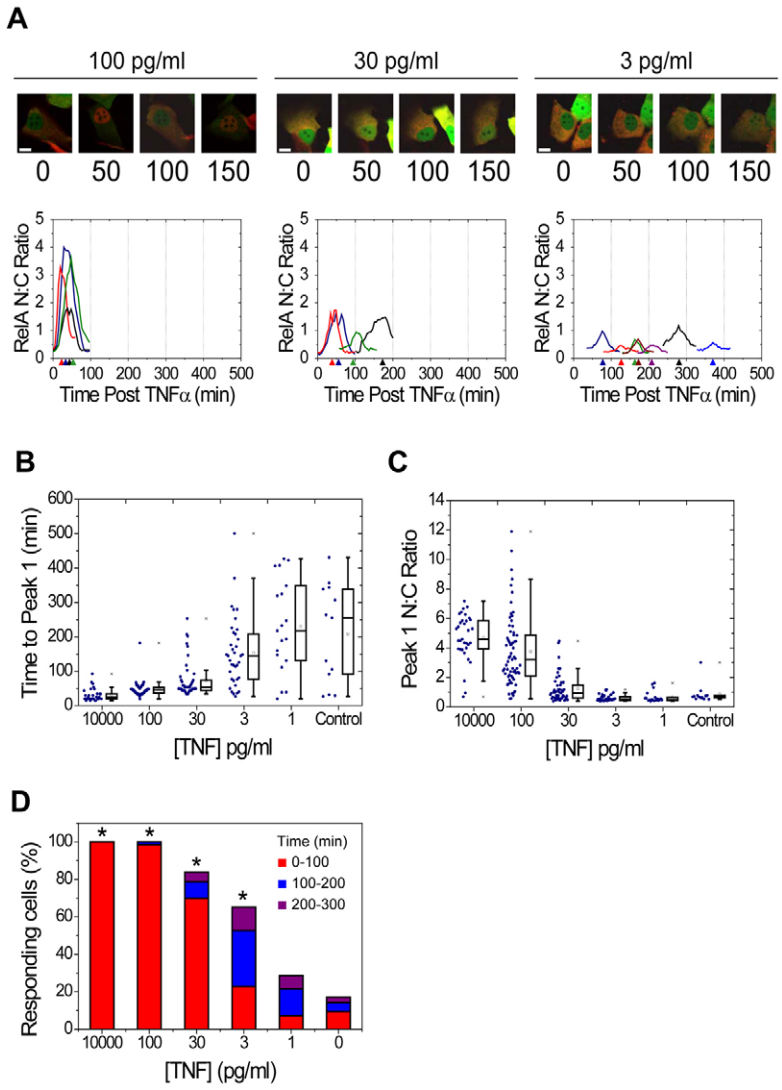

Fig. 2. Dose-dependent effects of TNFα on the amplitude and timing of the initial NF-κB nuclear translocation in single cells. SK-N-AS cells transiently transfected with RelA-dsRedxp and an empty-EGFP plasmid were stimulated with a range of TNFα doses and imaged by time-lapse confocal microscopy. (**A**) Time-course showing at least four representative cells following stimulation with high (100 pg/ml), intermediate (30 pg/ml) and low (3 pg/ml) doses of TNFα. The time to the peak (maximum) of the first RelA-dsRedxp nuclear translocation is indicated with arrowheads along the *x*-axes. Scale bar: 10 μm. (**B**) Box and whisker plot of the time to the first RelA-dsRedxp nuclear translocation (peak timing). There was no significant difference in the comparisons between 0, 1, 3 and 30 pg/ml. All other comparisons were significant ($P \leq 0.05$). (**C**) Box and whisker plot of the N:C amplitude following a range of TNFα doses. There was no significant difference in the comparisons between 0, 1, 3 and 30 pg/ml or between 100 pg/ml and 10 ng/ml. All other comparisons were significant ($P \leq 0.05$). Individual data points are shown to the left of each box. (**D**) Percentage of cells responding versus control as assessed by confocal microscopy. Colours denote the timing of the initial nuclear translocation occurring within 100 minutes (red), 100-200 minutes (blue) and 200-300 minutes (purple); *$P \leq 0.05$.

From these data (Fig. 2D), we calculated a Hill coefficient for co-operativity in dose-dependent pathway activation (see supplementary material Fig. S2F). The Hill coefficient was generated by plotting $\ln[\theta/(1-\theta)]$ against $\ln(\text{TNF}\alpha)$ for 1–100 pg/ml and estimating the slope of resulting linear trend, where θ corresponds to the percentage of responding cells (Fig. 2D) and TNFα corresponds to the dose. The data suggested a Hill coefficient of approximately 1, implying an absence of co-operativity in the mechanism of pathway activation (see supplementary material Fig. S2F).

It was shown previously that stimulation with 10 ng/ml TNFα elicited asynchronous N:C oscillations in SK-N-AS cells that maintained an average period of 100 minutes (Nelson et al., 2004). In other cell lines investigated, robust oscillations were also generated, albeit with some variation in period [e.g. shorter periods in mouse embryonic fibroblasts (Ashall et al., 2009) and rat pituitary GH3 cells (Friedrichsen et al., 2006)]. We therefore investigated whether lower doses would alter the period length or increase period variability. Surprisingly, it was found that regardless of the level of TNFα stimulation a robust 100 minute period was maintained (Fig. 3), suggesting that is a fundamental property of this system.

In summary, stimulation with high doses of TNFα resulted in synchronous initial RelA-dsRedxp translocation times with a high N:C amplitude, whereas lower doses generated reduced amplitudes and asynchronous response times. There was no difference in the amplitude or the timing of translocations at mock or low doses (0–3 pg/ml) but more cells responded to TNFα doses ≥3 pg/ml. Importantly, the amplitude of responses induced by very low doses was no different to that of the control, but the number of cells activated was increased, which might be functionally important in tissues.

The sustained presence of TNFα is required for NF-κB low-dose activation

Low TNFα doses (1–3 pg/ml) generated a random initial response time that was not significantly different from the unstimulated control (Fig. 2). At these low doses, it might be necessary for receptor activation events to occur above a threshold for a response to be generated (Lipniacki et al., 2007). To test this hypothesis, cells were exposed to a short pulse (5 minutes) at a range of TNFα concentrations. Stimulation with a 10 ng/ml pulse produced a single NF-κB nuclear translocation (Fig. 4A), as described previously (Nelson et al., 2004).

Stimulation with a range of TNFα doses (100 pg/ml, 1 ng/ml and 10 ng/ml) for a 5 minute pulse resulted in a significant (P≤0.05) dose-dependent reduction in the number of responding cells (Fig. 4B; see supplementary material Table S1B) compared with sustained stimulation (Fig. 2D). Doses of <10 ng/ml failed to activate the same proportion of cells as the equivalent dose at sustained stimulation (Fig. 2D). The most striking differences between sustained and pulsed treatment occurred after stimulation with 100 pg/ml TNFα (Fig. 4B vs Fig. 2D), where only ~30% of cells responded to a 5 minute pulse compared with 100% responding to sustained stimulation within 300 minutes (Fig. 4B, supplementary material Table S1B).

As the dissociation of TNFα from TNF-R1 has been reported to occur within 30 minutes and the internalisation half-time of the receptor complex has been reported to be between 10-20 minutes (Grell et al., 1998), it was considered unlikely that an initial 5 minute pulse determined responses after 50 minutes. We found that significantly fewer cells (P≤0.05) responded within 50 minutes (12.7±11.5%) after a 5 minute 100 pg/ml TNFα pulse than with sustained stimulation of the same dose (67.7±14.2%) (Fig. 4C vs Fig. 2A,B). There was no significant difference (P>0.05) between the N:C ratio of pulsed TNFα treatments and control cells at concentrations of <1 ng/ml (Fig. 4D). Furthermore, the method for medium replacement did not stress the cells, because there was no significant difference in the time to initial responses or the N:C ratio between a mock pulse or mock sustained stimulation (supplementary material Fig. S3A,B). In addition, estimation of a Hill coefficient from the data in Fig. 4B again suggested a lack of co-operativity in the pathway activation (supplementary material Fig. S3C)

Overall, following pulsed stimulation compared with sustained treatment with TNFα at and below 100 pg/ml the synchrony in timing of the first RelA-dsRedxp translocation was lost. Pulsed treatment also produced a N:C amplitude that was not significantly different between control and low-dose (1 or 3 pg/ml) TNFα stimulation. These data suggested that there was a threshold of activation, which required repetitive stimulation for system activation.

Evidence of a threshold of IκBα degradation with sustained TNFα stimulation

To understand how the delay to the first translocation was regulated, and to investigate the concept of a threshold of activation, we investigated the dynamic profiles of co-transfected IκBα-EGFP and RelA-dsRedxp in SK-N-AS cells (Fig. 5). In unstimulated conditions, we observed a basal turnover of IκBα-EGFP with a half-life of ~215 minutes [which was not significantly different (P>0.05) from the turnover of control EGFP protein at ~227

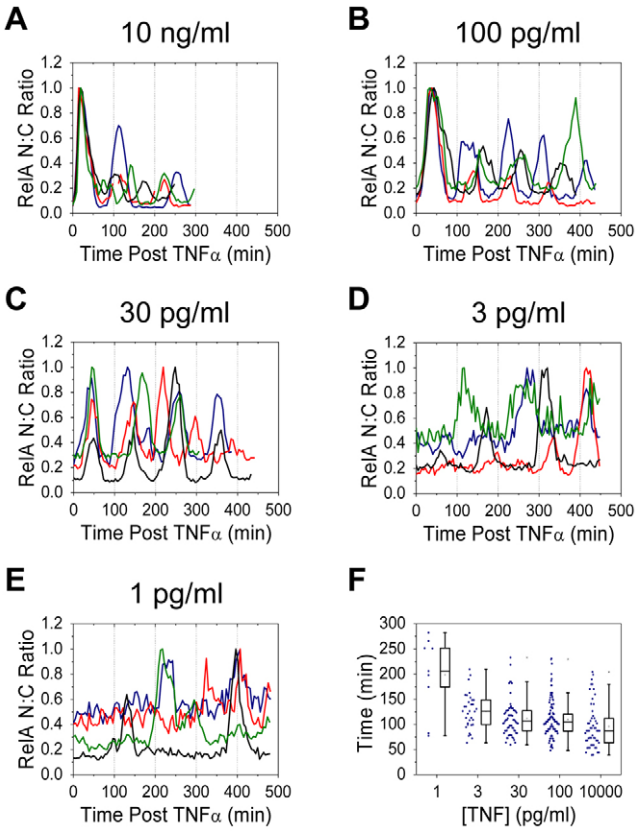

Fig. 3. Stimulation with a range of TNFα results in robust 100 minute oscillations. SK-N-AS cells transiently transfected with RelA-dsRedxp and an empty-EGFP plasmid, were stimulated with a range of TNFα concentrations. (**A-E**) Time-course showing four representative cells following sustained stimulation with high (10 ng/ml and 100 pg/ml), intermediate (30 pg/ml) and low (3 pg/ml and 1 pg/ml) doses of TNFα. Cell amplitudes are normalised to the maximum signal. (**F**) Box and whisker plots of the average peak-to-peak timing (period) of every oscillating cell per TNFα dose. Individual data points are shown to the left of each box.

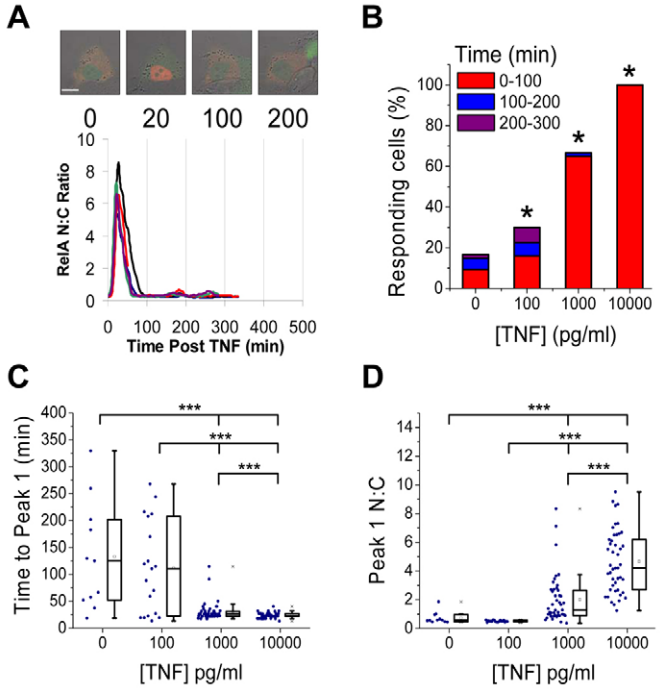

Fig. 4. Effect of TNFα pulse stimulation on amplitude and time of initial RelA-dsRedxp nuclear translocation. SK-N-AS cells transiently transfected with RelA-dsRedxp and an empty-EGFP plasmid were stimulated with a 5 minute pulse of TNFα at concentrations of 10 ng/ml, 1 ng/ml or 100 pg/ml, and imaged by time-lapse confocal microscopy. (**A**) Single-cell traces of five representative cells following 10 ng/ml TNFα are shown; time in minutes. Scale bar: 10 µm. (**B**) The percentage of cells responding, and (**C**) box and whisker plots of the time to initial response and (**D**) the amplitude of initial response for every cell responding was plotted following analysis. Individual data points are shown to left of each box in C and D. *P≤0.05 and ***P≤0.01.

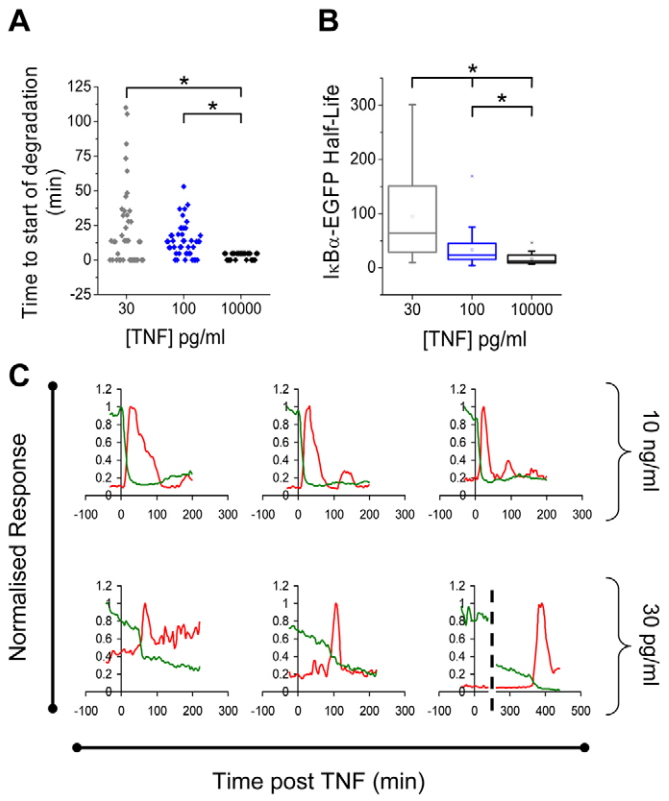

Fig. 5. The IκBα degradation profile suggests the presence of an upstream threshold of activation. SK-N-AS cells transiently transfected with RelA-dsRedxp and IκBα-EGFP plasmids were stimulated with 30 pg/ml, 100 pg/ml or 10 ng/ml TNFα. (**A**) The time to the initiation of IκBα-EGFP degradation and (**B**) IκBα-EGFP half-life at each dose were plotted. (**C**) Three representative single-cell traces stimulated with either 10 ng/ml (upper) or 30 pg/ml (lower) TNFα. The red line represents N:C ratio of RelA-dsRedxp and the green line represents total cellular IκBα-EGFP fluorescent levels (average intensity per pixel, normalised to their maximum respective signal). *$P \leq 0.05$.

minutes]. Stimulation with 10 ng/ml induced synchronous and rapid degradation of IκBα-EGFP with a half-life of ~16 minutes (Fig. 5). However, when cells were stimulated with lower TNFα concentrations, a different temporal profile was observed. There was a significant and apparently random time delay ($P \leq 0.05$) before IκBα-EGFP degradation was initiated, during which IκBα-EGFP continued to degrade with basal rate (Fig. 5A,C). Once initiated, the rate of IκBα-EGFP degradation was significantly increased (half-lifes of ~95 and ~33 minutes for 30 and 100 pg/ml, respectively) compared with the basal rate, which coincided with an onset of RelA-dsRedxp nuclear translocation. A significant difference ($P \leq 0.05$) in the IκBα-EGFP half-life of the cell population at different doses reflected the fact that only a partial degradation was observed at low doses, which correlated with lower amplitude of N:C RelA-dsRedxp translocation (Fig. 5B,C).

To quantify possible effects of different levels of RelA-dsRedxp and IκBα-EGFP expression, the time to the first RelA-dsRedxp response (supplementary material Fig. S4) and the RelA-dsRedxp N:C ratio (supplementary material Fig. S4) were analysed with respect to the intensity of the IκBα-EGFP for each TNFα concentration. There was a correlation between intensity of IκBα-EGFP and the time to the first RelA-dsRedxp response when the cells were stimulated with ≥100 pg/ml (supplementary material Fig. S4A,B), as seen previously (Nelson et al., 2004). However, this correlation was lost when cells were stimulated with 30 pg/ml TNFα (supplementary material Fig. S4C). The intensity of the IκBα-EGFP signal did not affect the amplitude of the initial response at 10 ng/ml, 100 pg/ml and 30 pg/ml TNFα (supplementary material Fig. S4).

Alterations to the existing mathematical model can simulate sustained oscillations and the delayed activation at low TNFα doses

Initially, we investigated whether existing mathematical models could capture the single-cell behaviour observed at low TNFα doses. Cheong and co-workers (Cheong et al., 2006) used ordinary differential equations based on the law of mass action, which were unable to simulate the intrinsic stochasticity of single cell responses. A theoretical model by Lipniacki and colleagues (Lipniacki et al., 2007) captured some heterogeneity of the system responses (in particular the random delay to the initial activation at low doses), by incorporating noise into the activation of TNF-R1 receptors and transcription of NF-κB feedback genes. However, this model could not predict the maintenance of the robust 100 minute oscillations or the reduction in the N:C amplitude that was observed in these experiments (Lipniacki et al., 2007).

Previously, we described a mathematical model that was capable of reproducing the single-cell data gathered from a number of experimental conditions (such as continuous and repeat pulse stimulation) (Ashall et al., 2009). In that model, we implemented a novel IKK module, which included IKK state recycling and negative feedback from A20 that allowed the experimental observations to be replicated in silico (Fig. 6A). In light of the dose-response data described above, we investigated whether this model could also simulate the following observations at low doses: (1) maintenance of robust 100 minute oscillations, (2) reduction of the RelA-dsRedxp N:C amplitude, and (3) a random delay to the first response, which is associated with a biphasic IκBα degradation profile.

We first investigated the ability of the model to maintain robust oscillations by decreasing parameter *TR* (Fig. 6A). (The model was developed for *TR*=1, which corresponds to 10 ng/ml TNFα.) Reduction of this parameter over successive orders of magnitude that simulated a reduction in the dose of TNFα, was unable to reproduce stable oscillations (Fig. 6A). We identified that a single modification in the IKK module (to remove the dependence of A20 inhibition on TNFα, and assume that A20 is constitutively active) produced a stable 100 minute period and a reduction in the N:C amplitude for lower *TR* values (Fig. 6B; supplementary material Table S2A,B). With this modification, the model still satisfactorily fitted all of the previous experimental observations (Fig. 6B). Detailed analysis indicated that whereas the original model generated a bifurcation point at a *TR* of 0.36 (a relatively high dose of 3.6 ng/ml) the modified IKK structure could shift the bifurcation point ten-times lower to a *TR* of 0.045 (Fig. 6C).

Our next aim was to explain the stochastic nature of the low-dose responses. Therefore, we developed a new stochastic model to provide a mechanistic hypothesis while making minimal biological assumptions (see Fig. 7). In particular, we have not tried to model the pathway upstream of IKK in detail because of the current lack of detailed understanding and quantitative data, but instead focused on a generic stochastic description of the activation of IKK which attempted to capture the degree of volatility caused by the incoming signals (modelled by *D* below). Whereas the

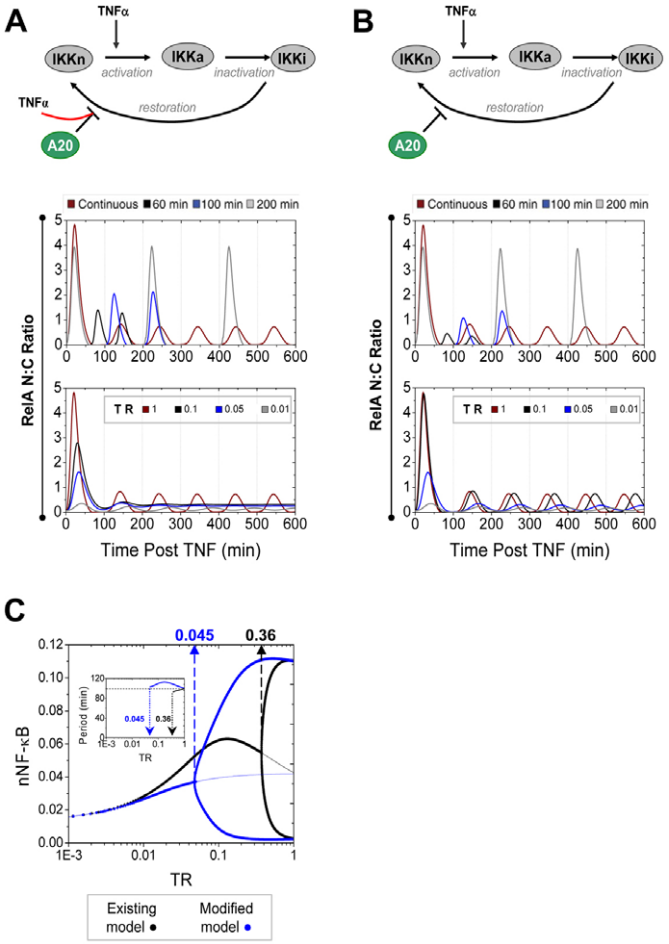

Fig. 6. A modified mathematical model can simulate sustained oscillations and the delayed activation at low TNFα doses. (**A**) The existing NF-κB model (Ashall et al., 2009). The structure of the IKK module (top), model simulations for continuous and repeat-pulse TNFα treatment (5 minute stimulation at 60, 100 and 200 minutes frequency, three times) (middle) and model simulations following a decrease in TNFα dose (decrease of *TR* from 1 to 0.01, bottom). (**B**) The modified model structure of the IKK module (after removal of the TNFα-dependence of A20 inhibition, top), model simulations for continuous and repeat pulsing (as in A) TNFα treatment (middle) and model simulations following a decrease in TNFα dose (decrease of *TR* from 1 to 0.01, below). (**C**) Bifurcation analysis (with respect to *TR*) of the existing (black) and the modified (blue) model. Shown are nuclear NF-κB levels in the steady state as a function of *TR* displaying a transition from a fixed point into a limit cycle at the bifurcation point, respectively for each model; insert presents the period of limit cycle oscillations as a function of *TR*.

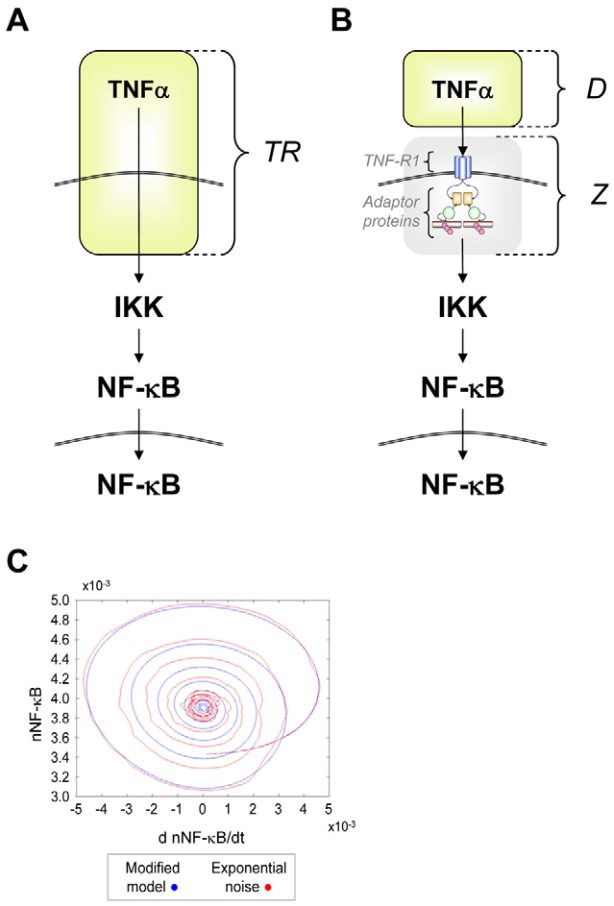

Fig. 7. Schematic representation of the steps of TNF-R1 signal transduction as encoded by the mathematical models. Noise can maintain 100 minute oscillation even below the deterministic oscillation threshold. (**A**) Schematic representation used in the previously described (Ashall et al., 2009) and modified model (as described in Fig. 6A and 6B, respectively). In these models, TR corresponds to a TNFα dose, which directly affects IKK activation. (**B**) Incorporation of the TNF-R1 transduction pathway. *D* represents the effective TNFα dose. *Z* represents the transduction process leading to IKK activation. (**C**) Phase plane representation [nuclear NF-κB(*t*) vs its time derivative] showing how the exponential noise of the stochastic model can maintain the 100 minute oscillations even when the modified model (blue) does not. The same initial conditions were used in both models (see supplementary material Table S2C).

previous model had used the single TNFα dose parameter *TR*, we next introduced a variable $Z(t)$, $(0 \leq Z << 1)$, such that for small time steps δt:

$$Z(t + \delta t) = Z(t)(1 - \rho)\delta t + D\,, \qquad (1)$$

where *D* is the effective TNFα (activation) dose and ρ is the inactivation rate, which describes the system's memory (supplementary material Table S2C). Time evolution of $Z(t)$ is represented by a first-order dynamical process representing the TNF-R1–IKK transduction pathway (Fig. 7B). For arbitrary values of ρ, we set *D* so that the response *Z* was equivalent to *TR* in the previous model (Fig. 6). The stochastic behaviour of the TNFα transduction pathway was modelled by taking *D* to be a random variable to be drawn from an appropriate distribution. Because such stochastic fluctuations continuously perturb the system, the model was able to induce persistent oscillations for lower TNFα doses than the equivalent deterministic model (see Fig. 7C for *D* randomised from exponential distribution).

The low-dose responses (Fig. 5C) were more accurately simulated when a heavy-tailed distribution for *D* was assumed. In Fig. 8A, single-cell RelA and IκBα trajectories are shown. These were generated using a memory parameter value $\rho = 0.07$ second^{-1} and a Pareto distribution (supplementary material Table S2C) in which the probability that *D* is greater than any value *d* decreases in a power-law fashion, i.e. $\Pr(D>d) = (\xi/d)^{\sigma}$ if $d>\xi$ ($\sigma=2$, $\xi=10^{-9}$). This exhibited stochastic NF-κB activation and ~100 minute

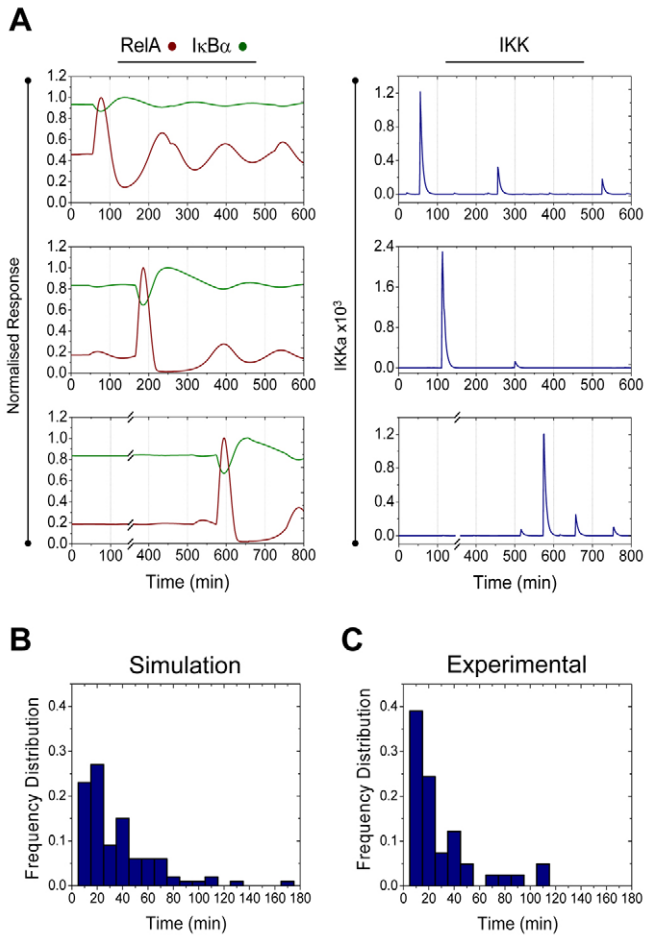

Fig. 8. A heavy-tail distribution for the effective TNFα dose can explain stochasticity of system activation at low TNFα doses. (**A**) Model simulations assuming noise-driven (Pareto-distributed effective dose *D*) kinetics of pathway activation (Eqn 1; supplementary material Table S2C). Three representative single-cell traces are shown: (left) N:C ratio of RelA (in red) and the total IκBα (in green) levels normalised to signal maximum, respectively. Corresponding active IKK trajectories are shown on the right. (**B**) Frequency distribution of the time to initiation of IκBα degradation assuming Pareto-distributed effective dose *D* (supplementary material Table S2C), calculated based on 100 simulated cells. (**C**) Frequency distribution of the time to initiation of IκBα-EGFP degradation following 30 pg/ml TNFα stimulation (calculated from data in Fig. 5A).

oscillations through stochastic excitation of the bifurcation point. Contrary to non-heavy-tailed distributions (e.g. exponential, supplementary material Fig. S5), a heavy-tailed Pareto distribution, in conjunction with a short-memory of signal transduction (high ρ), was able to generate dynamic trajectories of IKK levels (Fig. 8A right panel; supplementary material Table S2C) that allowed the simulation of the observed delay in single-cell activation. Based on this model it was possible to simulate initiation times of IκBα degradation that closely matched the measured distribution (Fig. 8B,C). To do this it was assumed that cells had a Pareto distribution with $\sigma=1.8$, $\xi=10^{-9}$ and included a threshold (defining system activation) that was four times the unstimulated value of active IKK.

Discussion

In this report, we used a combination of experimental and mathematical techniques to investigate the regulation of the NF-κB (RelA) transcription factor in single living SK-N-AS cells in response to physiological levels of TNFα. Previously, we and others showed that mammalian cells in response to saturating doses of TNFα (10 ng/ml) exhibited RelA oscillations with a period of approximately 100 minutes (Ashall et al., 2009; Friedrichsen et al., 2006; Nelson et al., 2004; Sung et al., 2009), and that this period could determine the pattern of downstream gene expression (Ashall et al., 2009). In the present study, we investigated whether the quantitative (timing, amplitude and oscillation frequency) characteristics of NF-κB responses were altered at low TNFα doses. Our data showed that single cells were not only able to oscillate in response to picomolar TNFα concentrations, but could also maintain a robust 100 minute period. This remarkable observation suggests that the maintenance of the 100 minute oscillation period in response to TNFα stimulation is a fundamental property of the NF-κB signalling system.

A study by Cheong and co-workers investigated NF-κB activation in response to a range of TNFα doses by using cell-population-based techniques such as gel retardation and IKK assays (Cheong et al., 2006). They showed that lowering the TNFα dose reduced the amount of nuclear NF-κB, yet maintained the same temporal profile regardless of the dose. Our data are fundamentally consistent with those of Cheong and colleagues (Cheong et al., 2006); however, our single-cell analyses demonstrate that cell populations are much more heterogeneous at lower doses of TNFα treatment. Our main observations are (1) a diminishing proportion of cells respond to decreasing doses of TNFα, (2) the N:C amplitude of the first translocation decreases with a reduction in the TNFα dose, (3) the responding cells display a stochastic delay in the time from stimulation to first observable RelA-dsRedxp nuclear translocation, and (4) the maintenance of a robust 100 minute period across all doses investigated. These data suggest that the decrease in population response observed by Cheong and colleagues was due to a combination of a smaller proportion of cells responding and a decrease in amplitude of single-cell responses, which were distributed in time.

The maintenance of robust NF-κB oscillations at a range of TNFα doses was interpreted in terms of our previously published mathematical model (Ashall et al., 2009). In that study, we identified the most generic model structure that could account for the available experimental data with fewest assumptions. Interestingly, we had previously been unable to discriminate between classes of models that invoked either TNFα-dependant or TNFα-independent inhibition via A20 feedback. With stimulation above a critical level, the previously used TNFα-dependent A20 inhibition model exhibited a stable-limit cycle with a period of approximately 100 minutes, to which the solutions converge (Fig. 6). This model could only support these stable NF-κB oscillations for high TNFα doses ($TR>0.36$; equivalent to 3.6 ng/ml TNFα). However, with a change in the structure of the IKK module (Fig. 6B) to invoke TNFα-independent A20 inhibition, the resulting model could maintain oscillations for doses approximately one-tenth of this concentration, and was still able to retain the ability to accurately simulate other stimulation conditions (Ashall et al., 2009). In both the current and modified models, the period length of the oscillations was largely independent of the stimulation level. This key observation suggests an important functional role for the conserved 100 minute NF-κB oscillations in response to widely

varying doses of TNFα. Our new experimental data also made a mechanistic prediction, by allowing us to discriminate between model structures for A20 action, which had been impossible to separate from previous data (Ashall et al., 2009). The low-dose TNFα data have therefore allowed us to make unexpected and non-intuitive predictions about the mechanism of A20 inhibition.

TNFα signalling through TNF-R1 receptors involves several steps where, following binding of trimeric TNFα to the receptor, adaptor proteins (TRAF2 and TRADD) are recruited to the receptor complex via their death domains (Hsu et al., 1996b; Hsu et al., 1995). RIP is then recruited and can ubiquitinate TRAF2 with Lys63 chains that serve as a scaffold for the IKK complex, allowing its activation (Hsu et al., 1996a; Zhang et al., 2000). Our current understanding is that in our experimental system at picomolar doses, the number of TNFα trimers available per cell is in the order of 100 molecules. This suggested that the heterogeneity of the low-dose responses could have originated from relatively small numbers of molecules at some point in the upstream signal transduction pathway, which might cause a downstream stochasticity in the number of activated IKK molecules. To analyse this mathematically, we developed a model that included stochasticity in transduction pathway leading from TNF-R1 receptor binding to IKK activation. The data suggest that the distribution of IKK activation events had to have heavy tails. Simulations with distributions with non-heavy tails (e.g. exponential distribution) did not give an appropriate activation distribution (Fig. 7C, Fig. 8; supplementary material Fig. S5), whereas heavy-tailed distributions, such as a Pareto distribution with memory, produced activation profiles that were similar to the data. It is possible that the large fluctuations seen with heavy tails are a result of processes such as receptor clustering or ligand passing from TNF-R2 to TNF-R1 (Liu et al., 2002; Tartaglia et al., 1993; Weiss et al., 1997). This model therefore describes a hypothetical and generic mechanism for generation of the observed stochastic dynamics without making unnecessary biological assumptions (Fig. 7).

Our next aim was to probe the mechanisms of NF-κB pathway activation responsible for the apparent all-or-nothing response, which was seen under low-dose stimulations. These responses are exhibited by the biphasic profiles of IκBα-EGFP level, which under low-dose stimulation exhibited a random but rapid transition from a low (basal; half-life, ~215 minutes) to a high degradation rate (~95 and ~33 minutes for 30 and 100 pg/ml respectively, Fig. 5C) coinciding with RelA-dsRedxp nuclear translocation. The stochasticity of the IκBα degradation initiation time increased with decreasing TNFα dose, and therefore implied that only a fraction of cells in the population responded within a fixed period of time. The input–output relationship (Hill coefficient of approximately 1 for sustained and 5 minute pulse stimulation) between the dose and the fraction of responding cells suggested a lack of co-operativity in the signal transduction pathway. It must be noted, however, that we cannot exclude the effect of background paracrine signalling. As shown by the ~18% of apparently responding cells in the absence of external stimulation, we did not attempt to test the responses of cells in a 'true zero stimulation'.

It has been suggested (using theoretical analysis) that the incidence and dynamics (amplitude and frequency) of NF-κB oscillations in response to TNFα activation might be significantly altered when RelA is overexpressed through transient transfection. This hypothesis arises from modelling predictions and from single time-point immunocytochemistry analysis on fixed cells (Barken et al., 2005; Cheong et al., 2009). We have previously provided experimental data to show that there is no correlation between the level of RelA-dsRedxp expression in transiently transfected cells (as used here) and the timing of oscillations in response to high level TNFα stimulation (Nelson et al., 2005). In the data shown in supplementary material Figs S1 and S2, we demonstrate that the level of fluorescent RelA and EGFP expression did not substantially affect the dynamics of NF-κB translocation at lower levels of TNFα stimulation. Several recent studies have shown similar dynamics of NF-κB oscillations when RelA is expressed at physiological (or close to physiological) levels. These include stably transfected cell lines (Ashall et al., 2009), cells infected with recombinant RelA expressing lentiviruses (Bartfeld et al., 2010; Lee et al., 2009), and MEFs from GFP-RelA knock-in mice (Sung et al., 2009). In addition, the recruitment of NF-κB subunits to various NF-κB-regulated promoters has been shown to be oscillatory (Ashall et al., 2009; Sun et al., 2008b) and oscillations in gene expression have also been reported in untransfected primary macrophages following stimulation with TNFα (Sun et al., 2008a). Together, these studies support the view that moderate variation in RelA expression level does not substantially affect oscillation incidence or dynamics.

During the inflammatory response, cells participate in two regulatory processes; the first concerns the fate of individual cells (commitment to apoptosis or transition through the cell cycle) in response to cytokine stimulation. The second relates to the production of NF-κB-responsive cytokines and chemokines, which enables propagation of the inflammatory signal. These physiological processes have often been interpreted as resulting from a population of cells that display homogenous responses with dose-dependent amplitudes. Although there were some dose-dependant amplitude changes, our current analysis suggests, by contrast, that the population response arises mainly from individual cells exhibiting stochastic all-or-nothing responses with random timing. Thus, the dose-dependent control of population-level dynamics is mainly achieved by regulating the number of responding cells. This strategy might be beneficial for cell signalling systems because responding cells are fully activated, thereby avoiding potential ambiguity during crucial decision-making processes. We therefore suggest that in the NF-κB system, robust oscillations with a defined period are a standard response to constant TNFα stimulation. However, at the local level, cells might well be exposed to fluctuating TNFα levels, which we have previously shown can force different NF-κB translocation frequencies and result in altered gene expression (Ashall et al., 2009). We propose that the system response allows a robust and consistent (potentially all-or-nothing) gene expression profile to be generated in each responding cell. The response to lower levels of signal results in lower proportions of responding cells. This suggests that further development of models for cellular communication and propagation of inflammatory signals between cells should be a priority to allow a better understanding of the tissue-level switch between amplification and resolution of inflammation. Recent data (Paszek et al., 2010) has suggested that cell-to-cell heterogeneity is an intrinsic feature of the NF-κB system. Therefore, the variability in response to low-dose stimulation might also be a fundamental property of the NF-κB inflammatory response.

Materials and Methods

Plasmids

All plasmids were propagated in *E. coli* DH5α and purified using Maxiprep kits (Qiagen). NF-Luc (pNF-κB-Luc, Stratagene) contains five repeats of an NF-κB-sensitive enhancer element upstream of the TATA box, controlling expression of

luciferase. pIκBα-Luc contains nucleotides –332 to +35 of the human gene promoter driving the expression of luciferase and was a kind gift from the laboratory of Ron Hay (University of Dundee, Dundee, UK). pEGFP-N1 was from Clontech. The RelA-dsRedxp construct was previously described (Nelson et al., 2002) and contains the dsRedxp fluorescent protein (Clontech) fused to the C-terminus of RelA.

Cell culture

Human S-type neuroblastoma cells (SK-N-AS, ECACC No. 94092302) were grown in minimal essential medium (MEM) with Earle's salts (Gibco) supplemented with 10% (v/v) foetal bovine serum (FBS) (Harlan Seralab) and 1% (v/v) non-essential amino acids (NEAA) (Gibco), cultured at 37°C in 5% CO_2 and grown to 80% confluency.

Treatment of cells with TNFα

Recombinant TNFα stock (10 μg/ml; Calbiochem) was diluted in series in serum-free MEM and was then added to the dish at the appropriate concentration. A mock stimulation was performed in control experiments using serum-free MEM. For the luciferase reporter assay, TNFα was added at the beginning of the experiment. For confocal fluorescence microscopy, TNFα was added 30 minutes after the experiment had begun to record the basal fluorescent signals.

Luciferase reporter assay

SK-N-AS cells were grown in 24-well plates (6×10^4 cells per well) and transiently transfected with the appropriate plasmid using FuGene6 (Boehringer Mannheim) at the optimised FuGene6:DNA ratio of 2:1 following manufacturer's instructions. Experiments were performed 24 hours after transfection and stimulated with the required TNFα dose for the times stated. Cells were washed once with ice-cold PBS and lysates [0.025% (w/v) dithiothreitol, 1% BSA, 1% Triton X-100, 15% glycerol, 0.1 mM EDTA, 8 mM $MgCl_2$, in H_2O] were prepared. Luciferase activity was measured using a PerkinElmer Envision luminometer. Experiments were performed three times and expressed as the average fold-change for each treatment ± s.e.m.

Fluorescence microscopy

SK-N-AS cells (1.6×10^5) were seeded in 35 mm glass-bottom dishes in 3 ml medium. Cells were co-transfected after 24 hours with RelA-dsRedxp and either with pEGFP-N1 or IκBα-EGFP, as described above. Confocal microscopy was carried out 24 hours after transfection in a humidified CO_2 incubator (37°C, 5% CO_2) using a Zeiss LSM510 on a Carl Zeiss Axiovert 200M with a 63× 1.4 NA DIC oil-immersion objective. dsRedxp was excited with a 543 nm green Helium Neon laser and detected through a 570 nm long-pass filter. Excitation of EGFP was carried out with a 488 nm Argon ion laser, and emitted light was reflected through a 505–550 nm band-pass filter from a 540 nm dichroic mirror. Data were captured using AutoTimeSerie Macro v1.18 (Rabut and Ellenberg, 2004). Cells were treated with the appropriate stimulation 30 minutes following the onset of time-lapse imaging and images captured every 5 minutes for at least 5 hours. Data were analysed using CellTracker (Shen et al., 2006) by exporting mean fluorescence ratios from the whole of the cytoplasmic and nuclear boundaries for each cell and expressing this as a nuclear to cytoplasmic (N:C) ratio. The average and standard deviation of the N:C ratio from the 30 minute pre-stimulation period were calculated and a threshold set which was two standard deviations above pre-stimulation average; an NF-κB response was characterised as being a transient rise in N:C ratio with more than three data points above this threshold (Jameson et al., 2009).

Mathematical modelling

In this work, we modified our previously described two-feedback model of NF-κB signalling (see supplementary material Table S2) (Ashall et al., 2009). Mathematical models were implemented and simulated in Matlab R2009a environment (including Statistics Toolbox). Bifurcation analysis was performed with the numerical package XPPAUT (Ermentrout, 2002).

Statistical analysis

Statistical tests between different treatments were performed by the non-parametric Kruskal–Wallis test with Bonferroni adjustment for multiple comparisons. When comparing proportions of responding cells in reporter assays, one-way ANOVA followed by a Fischer's test was used. All tests were performed at 0.05 significance level and performed using Minitab 15 (Minitab Solutions, UK) statistical software.

We thank Ron Hay (University of Dundee, UK) for the kind gift of the IκBα-Luc vector. We also thank D. Broomhead, D. Kell and M. Muldoon (University of Manchester, UK) for useful discussions. The work was funded by Biotechnology and Biological Sciences Research Council (BBSRC) and Engineering Physical Sciences Research Council (EPSRC) grants BBD0107481/BBD0088081 and BBF0059381/BBF0058141/BBF00561X1, GR/S29256/01 and Medical Research Council (MRC) grant G0500346. D.A.T. is funded by a BBSRC PhD studentship. C.V.H. was funded by The Professor John Glover Memorial Postdoctoral Fellowship. D.A.R. held an Engineering Physical Sciences Research Council (EPSRC) Senior Fellowship (GR/S29256/01), and his work was also funded by the European Union BIOSIM Network Contract 005137. The Centre for Cell Imaging has been supported through BBSRC REI grant BBE0129651. Carl Zeiss Limited provided technical support. Deposited in PMC for release after 6 months. This article is freely accessible online from the date of publication.

Supplementary material available online at
http://jcs.biologists.org/cgi/content/full/123/16/2834/DC1

References

Aggarwal, B. B. (2000). Tumour necrosis factors receptor associated signalling molecules and their role in activation of apoptosis, JNK and NF-kappaB. *Ann. Rheum. Dis.* **59 Suppl 1**, i6-i16.

Ashall, L., Horton, C. A., Nelson, D. E., Paszek, P., Harper, C. V., Sillitoe, K., Ryan, S., Spiller, D. G., Unitt, J. F., Broomhead, D. S. et al. (2009). Pulsatile stimulation determines timing and specificity of NF-kappaB-dependent transcription. *Science* **324**, 242-246.

Barken, D., Wang, C. J., Kearns, J., Cheong, R., Hoffmann, A. and Levchenko, A. (2005). Comment on "Oscillations in NF-kappaB signaling control the dynamics of gene expression". *Science* **308**, 52.

Bartfeld, S., Hess, S., Bauer, B., Machuy, N., Ogilvie, L., Schuchhardt, J. and Meyer, T. (2010). High-throughput and single-cell imaging of NF-kappaB oscillations using monoclonal cell lines. *BMC Cell Biol.* **11**, 21.

Berridge, M. J., Bootman, M. D. and Lipp, P. (1998). Calcium – a life and death signal. *Nature* **395**, 645-648.

Butera, S. T., Roberts, B. D. and Folks, T. M. (1996). Ligand passing by the p75 tumour necrosis factor receptor enhances HIV-1 activation. *Cytokine* **8**, 745-750.

Cheong, R., Bergmann, A., Werner, S. L., Regal, J., Hoffmann, A. and Levchenko, A. (2006). Transient IkappaB kinase activity mediates temporal NF-kappaB dynamics in response to a wide range of tumor necrosis factor-alpha doses. *J. Biol. Chem* **281**, 2945-2950.

Cheong, R., Wang, C. J. and Levchenko, A. (2009). High content cell screening in a microfluidic device. *Mol. Cell Proteomics* **8**, 433-442.

Coward, W. R., Okayama, Y., Sagara, H., Wilson, S. J., Holgate, S. T. and Church, M. K. (2002). NF-kappa B and TNF-alpha: a positive autocrine loop in human lung mast cells? *J. Immunol.* **169**, 5287-5293.

Damas, P., Reuter, A., Gysen, P., Demonty, J., Lamy, M. and Franchimont, P. (1989). Tumor necrosis factor and interleukin-1 serum levels during severe sepsis in humans. *Crit. Care Med.* **17**, 975-978.

Dolmetsch, R. E., Lewis, R. S., Goodnow, C. C. and Healy, J. I. (1997). Differential activation of transcription factors induced by Ca2+ response amplitude and duration. *Nature* **386**, 855-858.

Dolmetsch, R. E., Xu, K. and Lewis, R. S. (1998). Calcium oscillations increase the efficiency and specificity of gene expression. *Nature* **392**, 933-936.

Ermentrout, B. (2002). *Simulating, Analyzing, and Animating Dynamical Systems: A Guide to XPPAUT for Researchers and Students.* Philadelphia, PA: SIAM.

Friedrichsen, S., Harper, C. V., Semprini, S., Wilding, M., Adamson, A. D., Spiller, D. G., Nelson, G., Mullins, J. J., White, M. R. and Davis, J. R. (2006). Tumor necrosis factor-alpha activates the human prolactin gene promoter via nuclear factor-kappaB signaling. *Endocrinology* **147**, 773-781.

Grell, M., Wajant, H., Zimmermann, G. and Scheurich, P. (1998). The type 1 receptor (CD120a) is the high-affinity receptor for soluble tumor necrosis factor. *Proc. Natl. Acad. Sci. USA* **95**, 570-575.

Hayden, M. S. and Ghosh, S. (2008). Shared principles in NF-kappaB signaling. *Cell* **132**, 344-362.

Hsu, H., Xiong, J. and Goeddel, D. V. (1995). The TNF receptor 1-associated protein TRADD signals cell death and NF-kappa B activation. *Cell* **81**, 495-504.

Hsu, H., Huang, J., Shu, H. B., Baichwal, V. and Goeddel, D. V. (1996a). TNF-dependent recruitment of the protein kinase RIP to the TNF receptor-1 signaling complex. *Immunity* **4**, 387-396.

Hsu, H., Shu, H. B., Pan, M. G. and Goeddel, D. V. (1996b). TRADD-TRAF2 and TRADD-FADD interactions define two distinct TNF receptor 1 signal transduction pathways. *Cell* **84**, 299-308.

Jameson, D., Turner, D. A., Ankers, J., Kennedy, S., Ryan, S., Swainston, N., Griffiths, T., Spiller, D. G., Oliver, S. G., White, M. R. et al. (2009). Information management for high content live cell imaging. *BMC Bioinformatics* **10**, 226.

Khabar, K. S., Siddiqui, S. and Armstrong, J. A. (1995). WEHI-13VAR: a stable and sensitive variant of WEHI 164 clone 13 fibrosarcoma for tumor necrosis factor bioassay. *Immunol. Lett.* **46**, 107-110.

Lee, T. K., Denny, E. M., Sanghvi, J. C., Gaston, J. E., Maynard, N. D., Hughey, J. J. and Covert, M. W. (2009). A noisy paracrine signal determines the cellular NF-kappaB response to lipopolysaccharide. *Sci. Signal.* **2**, ra65.

Lipniacki, T., Puszynski, K., Paszek, P., Brasier, A. R. and Kimmel, M. (2007). Single TNFalpha trimers mediating NF-kappaB activation: stochastic robustness of NF-kappaB signaling. *BMC Bioinformatics* **8**, 376.

Liu, Y., Xu, L., Opalka, N., Kappler, J., Shu, H. B. and Zhang, G. (2002). Crystal structure of sTALL-1 reveals a virus-like assembly of TNF family ligands. *Cell* **108**, 383-394.

Matalka, K. Z., Tutunji, M. F., Abu-Baker, M. and Abu Baker, Y. (2005). Measurement of protein cytokines in tissue extracts by enzyme-linked immunosorbent assays:

application to lipopolysaccharide-induced differential milieu of cytokines. *Neuro. Endocrinol. Lett.* **26**, 231-236.

Nakai, Y., Hamagaki, S., Takagi, R., Taniguchi, A. and Kurimoto, F. (1999). Plasma concentrations of tumor necrosis factor-alpha (TNF-alpha) and soluble TNF receptors in patients with anorexia nervosa. *J. Clin. Endocrinol. Metab.* **84**, 1226-1228.

Nelson, D. E., Ihekwaba, A. E., Elliott, M., Johnson, J. R., Gibney, C. A., Foreman, B. E., Nelson, G., See, V., Horton, C. A., Spiller, D. G. et al. (2004). Oscillations in NF-kappaB signaling control the dynamics of gene expression. *Science* **306**, 704-708.

Nelson, D. E., Horton, C. A., See, V., Johnson, J. R., Nelson, G., Spiller, D. G., Kell, D. B. and White, M. R. H. (2005). Response to comment on "Oscillations in NF-kappaB signaling control the dynamics of gene expression". *Science* **308**, 52b.

Nelson, G., Paraoan, L., Spiller, D. G., Wilde, G. J. C., Browne, M. A., Djali, P. K., Unitt, J. F., Sullivan, E., Floettmann, E. and White, M. R. H. (2002). Multi-parameter analysis of the kinetics of NF-kappaB signalling and transcription in single living cells. *J. Cell Sci.* **115**, 1137-1148.

Paszek, P., Ryan, S., Ashall, L., Sillitoe, K., Harper, C. V., Spiller, D. G., Rand, D. A. and White, M. R. H. (2010). Population robustness arising from cellular heterogeneity. *Proc. Natl. Acad. Sci. USA* **107**, 11644-11649.

Rabut, G. and Ellenberg, J. (2004). Automatic real-time three-dimensional cell tracking by fluorescence microscopy. *J. Microsc.* **216**, 131-137.

Shen, H., Nelson, G., Nelson, D. E., Kennedy, S., Spiller, D. G., Griffiths, T., Paton, N., Oliver, S. G., White, M. R. and Kell, D. B. (2006). Automated tracking of gene expression in individual cells and cell compartments. *J. R. Soc. Interface* **3**, 787-794.

Sun, L., Yang, G., Zaidi, M. and Iqbal, J. (2008a). TNF-induced gene expression oscillates in time. *Biochem. Biophys. Res. Commun.* **371**, 900-905.

Sun, L., Yang, G., Zaidi, M. and Iqbal, J. (2008b). TNF-induced oscillations in combinatorial transcription factor binding. *Biochem. Biophys. Res. Commun.* **371**, 912-916.

Sung, M. H., Salvatore, L., De Lorenzi, R., Indrawan, A., Pasparakis, M., Hager, G. L., Bianchi, M. E. and Agresti, A. (2009). Sustained oscillations of NF-kappaB produce distinct genome scanning and gene expression profiles. *PLoS ONE* **4**, e7163.

Tartaglia, L. A., Pennica, D. and Goeddel, D. V. (1993). Ligand passing: the 75-kDa tumor necrosis factor (TNF) receptor recruits TNF for signaling by the 55-kDa TNF receptor. *J. Biol. Chem.* **268**, 18542-18548.

Weiss, T., Grell, M., Hessabi, B., Bourteele, S., Muller, G., Scheurich, P. and Wajant, H. (1997). Enhancement of TNF receptor p60-mediated cytotoxicity by TNF receptor p80: requirement of the TNF receptor-associated factor-2 binding site. *J. Immunol.* **158**, 2398-2404.

Zandi, E., Chen, Y. and Karin, M. (1998). Direct phosphorylation of IkappaB by IKKalpha and IKKbeta: discrimination between free and NF-kappaB-bound substrate. *Science* **281**, 1360-1363.

Zhang, S. Q., Kovalenko, A., Cantarella, G. and Wallach, D. (2000). Recruitment of the IKK signalosome to the p55 TNF receptor: RIP and A20 bind to NEMO (IKKgamma) upon receptor stimulation. *Immunity* **12**, 301-311.

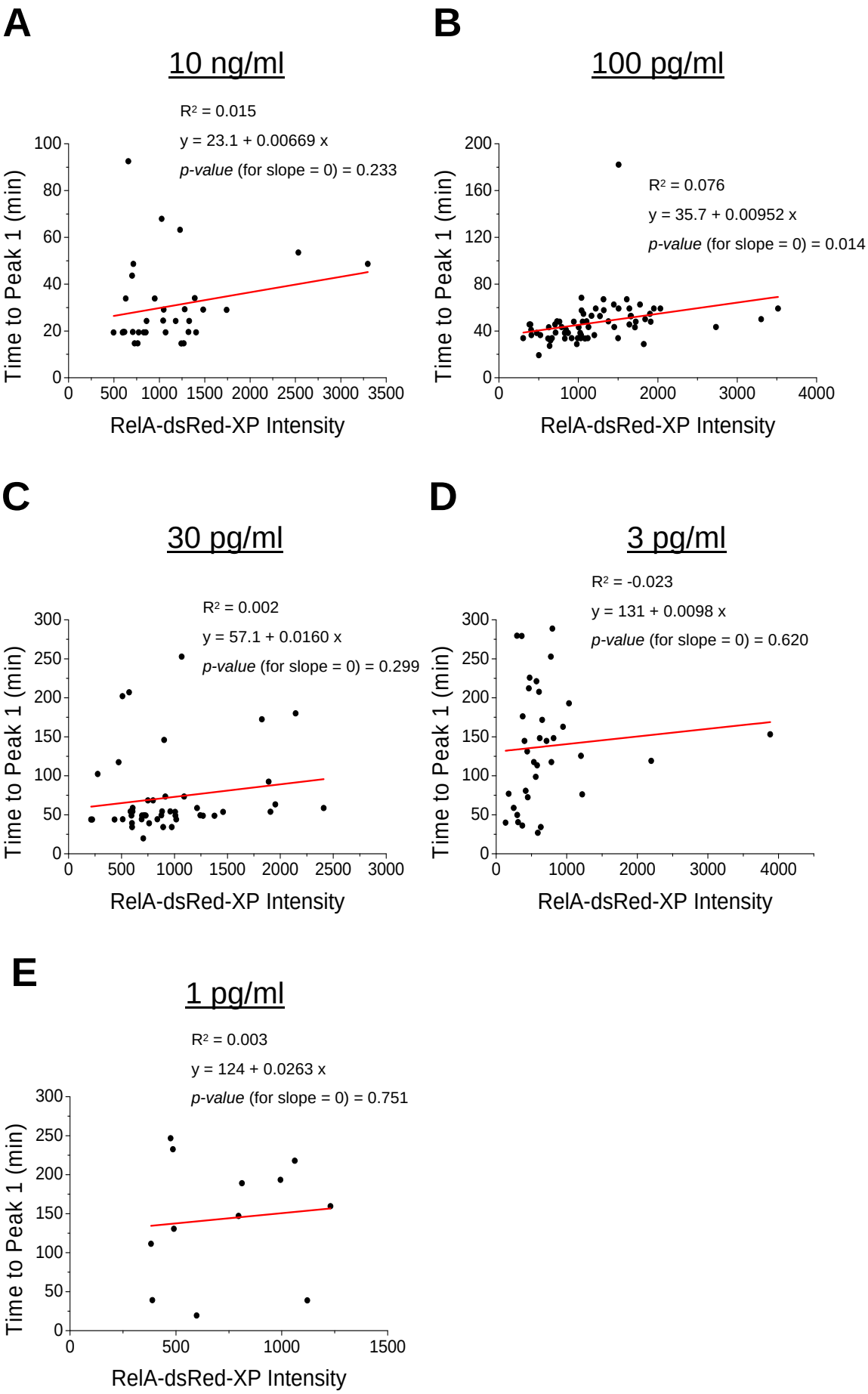
A
10 ng/ml
R² = 0.015
y = 23.1 + 0.00669 x
p-value (for slope = 0) = 0.233
Time to Peak 1 (min)
RelA-dsRed-XP Intensity
B
100 pg/ml
R² = 0.076
y = 35.7 + 0.00952 x
p-value (for slope = 0) = 0.014
Time to Peak 1 (min)
RelA-dsRed-XP Intensity
C
30 pg/ml
R² = 0.002
y = 57.1 + 0.0160 x
p-value (for slope = 0) = 0.299
Time to Peak 1 (min)
RelA-dsRed-XP Intensity
D
3 pg/ml
R² = -0.023
y = 131 + 0.0098 x
p-value (for slope = 0) = 0.620
Time to Peak 1 (min)
RelA-dsRed-XP Intensity
E
1 pg/ml
R² = 0.003
y = 124 + 0.0263 x
p-value (for slope = 0) = 0.751
Time to Peak 1 (min)
RelA-dsRed-XP Intensity

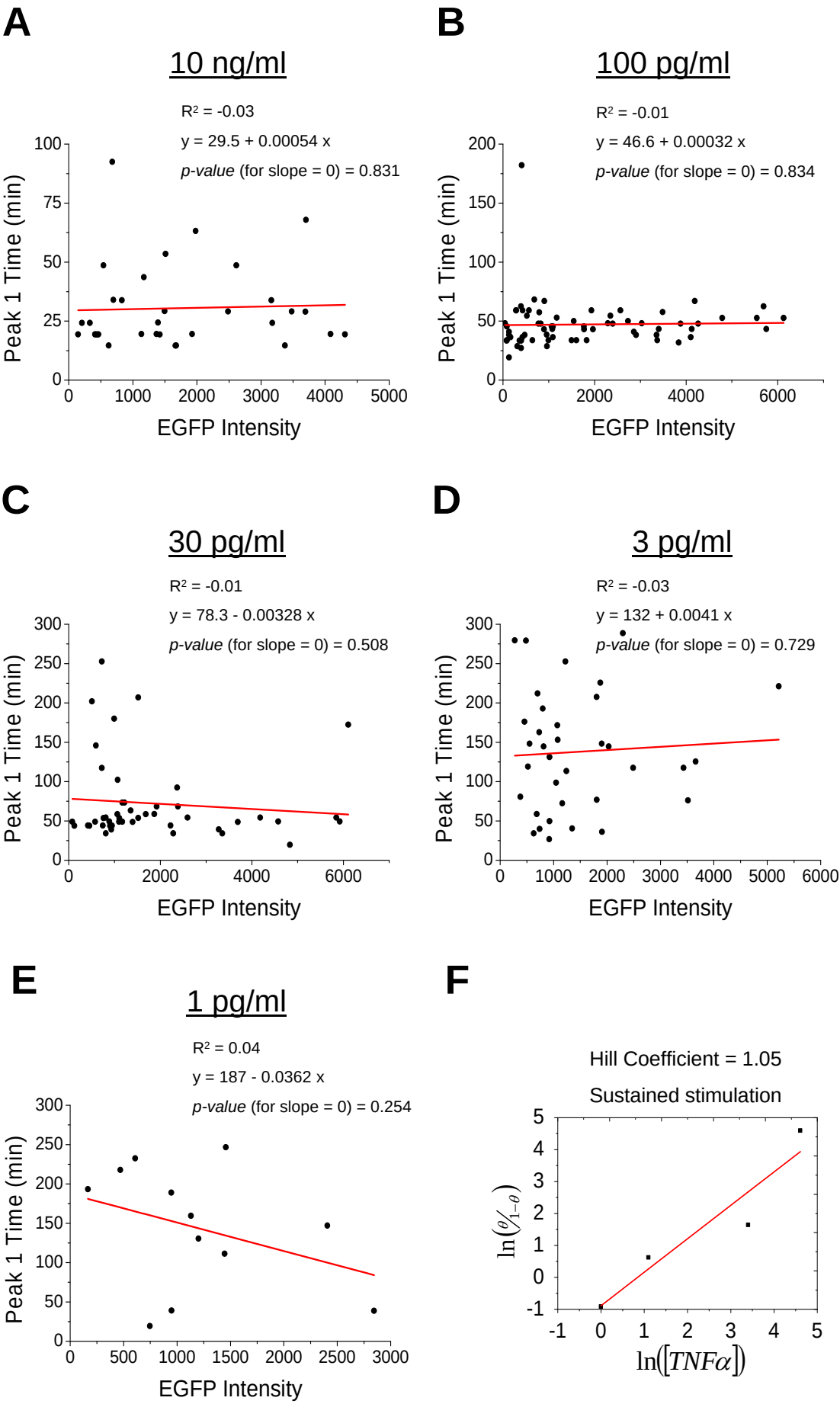
A
10 ng/ml
R² = -0.03
y = 29.5 + 0.00054 x
p-value (for slope = 0) = 0.831
Peak 1 Time (min)
EGFP Intensity
B
100 pg/ml
R² = -0.01
y = 46.6 + 0.00032 x
p-value (for slope = 0) = 0.834
Peak 1 Time (min)
EGFP Intensity
C
30 pg/ml
R² = -0.01
y = 78.3 - 0.00328 x
p-value (for slope = 0) = 0.508
Peak 1 Time (min)
EGFP Intensity
D
3 pg/ml
R² = -0.03
y = 132 + 0.0041 x
p-value (for slope = 0) = 0.729
Peak 1 Time (min)
EGFP Intensity
E
1 pg/ml
R² = 0.04
y = 187 - 0.0362 x
p-value (for slope = 0) = 0.254
Peak 1 Time (min)
EGFP Intensity
F
Hill Coefficient = 1.05
Sustained stimulation
ln(θ/(1−θ))
ln([TNFα])

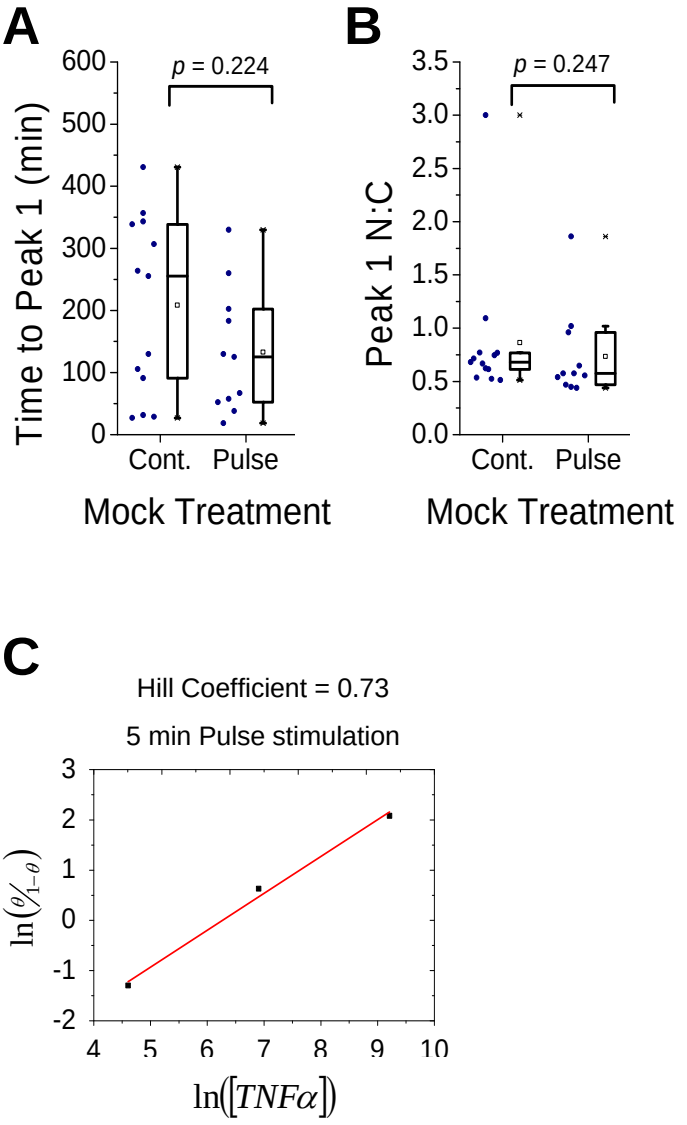
A
Time to Peak 1 (min)
600
500
400
300
200
100
0
p = 0.224
Cont.
Pulse
Mock Treatment
B
Peak 1 N:C
3.5
3.0
2.5
2.0
1.5
1.0
0.5
0.0
p = 0.247
Cont.
Pulse
Mock Treatment
C
Hill Coefficient = 0.73
5 min Pulse stimulation
3
2
1
0
-1
-2
4
5
6
7
8
9
10
ln(θ/1−θ)
ln([TNFα])

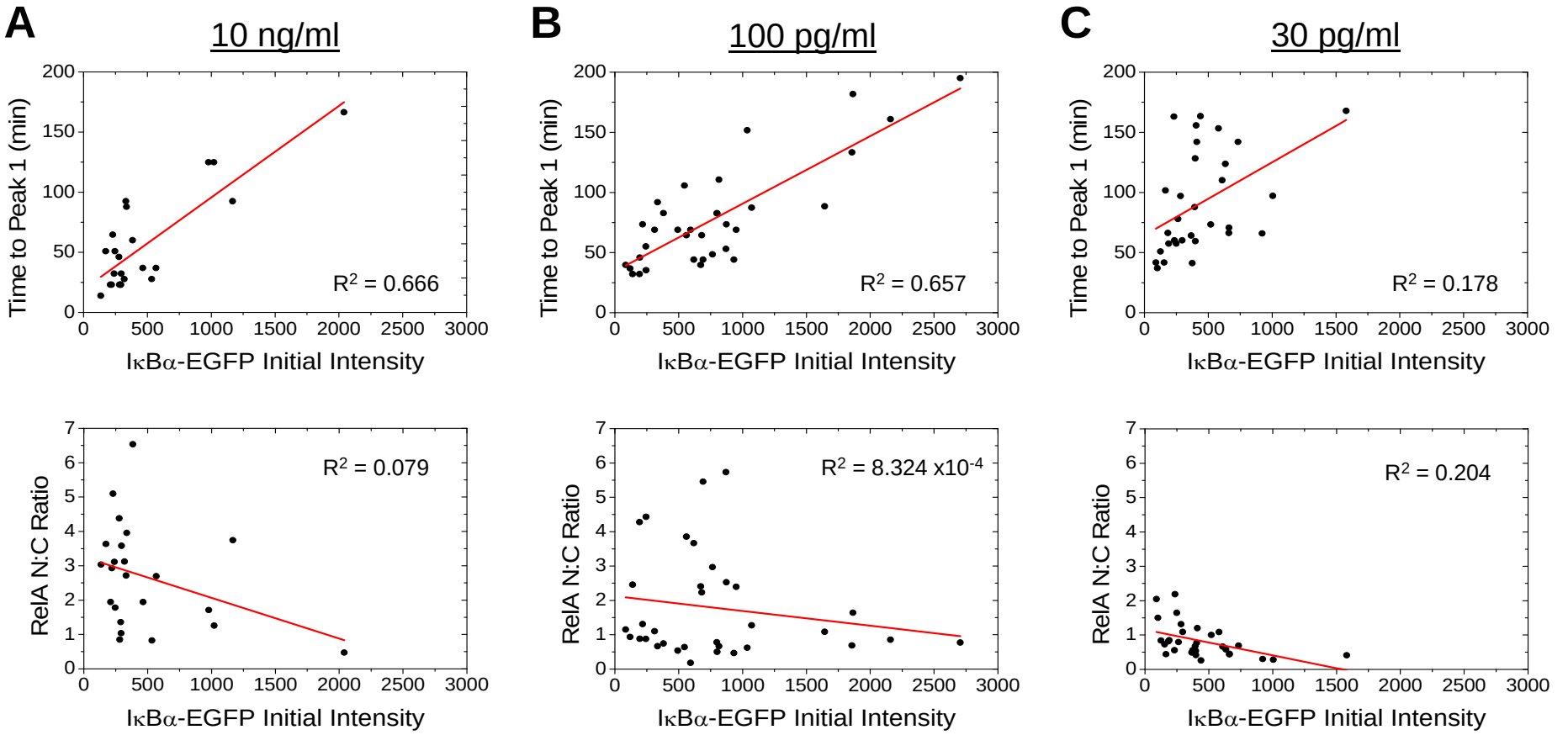
A
10 ng/ml
B
100 pg/ml
C
30 pg/ml
Time to Peak 1 (min)
IκBα-EGFP Initial Intensity
R2 = 0.666
R2 = 0.657
R2 = 0.178
RelA N:C Ratio
R2 = 0.079
R2 = 8.324 x10-4
R2 = 0.204

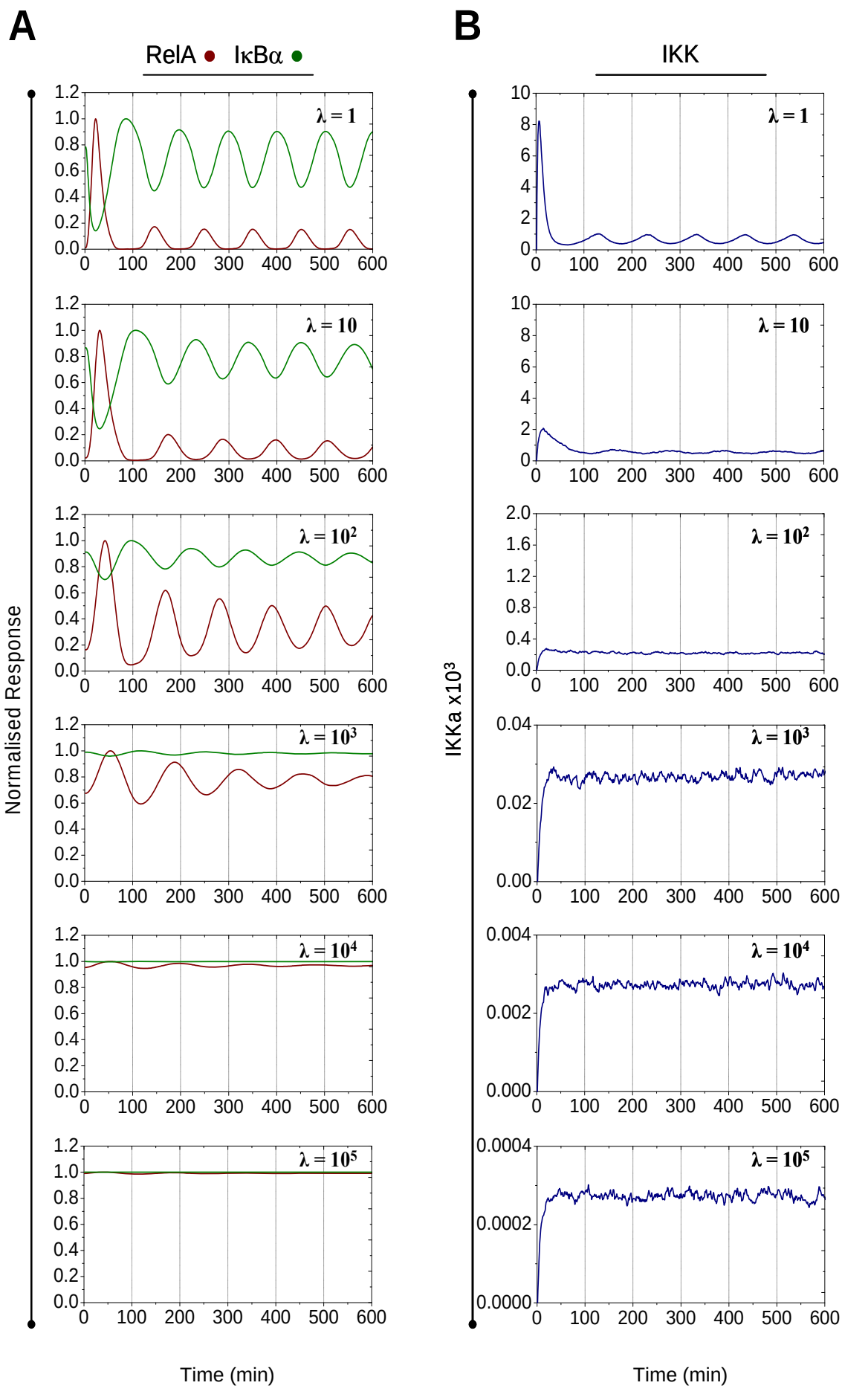
A
RelA
IκBα
B
IKK
Normalised Response
IKKa x10³
λ = 1
λ = 10
λ = 10²
λ = 10³
λ = 10⁴
λ = 10⁵
Time (min)
Time (min)

Supplementary Table S1

Percentage of responding cells at various doses of TNFα.

A

Dose (pg/ml)	% Respond (± S.D.)	Total No. of Cells	No. of Experiments
0	18.95 (± 17.1)	47	3
1	28.57 (± 10.4)	41	3
3	65.15 (± 22.4)	51	3
30	83.78 (± 4.21)	55	3
100	100 (± 0.00)	67	3
10000	100 (± 0.00)	33	3

B

Dose (pg/ml)	% Respond (± S.D.)	Total No. of Cells	No. of Experiments
0	16.62 (± 9.27)	57	3
100	38.48 (± 5.17)	49	3
1000	98.15 (± 3.21)	47	3
10000	100 (± 0.00)	45	3

Supplementary Table S2

Mathematical description of NF-κB signalling.

A

$$\frac{d}{dt} IKKn(t) = kp \times \frac{kbA20}{kbA20 + A20(t)} \times IKKi(t) - TR \times ka \times IKKn(t) \quad \text{(A1)}$$

$$\frac{d}{dt} IKKa(t) = TR \times ka \times IKKn(t) - ki \times IKKa(t) \quad \text{(A2)}$$

$$\frac{d}{dt} IKKi(t) = ki \times IKKa(t) - kp \times \frac{kbA20}{kbA20 + A20(t)} \times IKKi(t) \quad \text{(A3)}$$

$$\frac{d}{dt} NF\kappa B(t) = kd1a \times (I\kappa B\alpha \circ NF\kappa B)(t) - ka1a \times I\kappa B\alpha(t) \times NF\kappa B(t) - ki1 \times NF\kappa B(t) + ke1 \times nNF\kappa B(t) + kt2a \times (pI\kappa B\alpha \circ NF\kappa B)(t) + c5a \times (I\kappa B\alpha \circ NF\kappa B)(t) \quad \text{(A4)}$$

$$\frac{d}{dt} nNF\kappa B(t) = kd1a \times (nI\kappa B\alpha \circ nNF\kappa B)(t) - ka1an \times nI\kappa B\alpha(t) \times nNF\kappa B(t) + ki1 \times kv \times NF\kappa B(t) - ke1 \times kv \times nNF\kappa B(t) \quad \text{(A5)}$$

$$\frac{d}{dt} I\kappa B\alpha(t) = kd1a \times (I\kappa B\alpha \circ NF\kappa B)(t) - ka1a \times I\kappa B\alpha(t) \times NF\kappa B(t) + c2a \times tI\kappa B\alpha(t) - c4a \times I\kappa B\alpha(t) - ki3a \times I\kappa B\alpha(t) + ke3a \times nI\kappa B\alpha(t) - kc1a \times IKKa(t) \times I\kappa B\alpha(t) \quad \text{(A6)}$$

$$\frac{d}{dt} nI\kappa B\alpha(t) = kd1a \times (nI\kappa B\alpha \circ nNF\kappa B)(t) - ka1an \times nI\kappa B\alpha(t) \times nNF\kappa B(t) - c4a \times nI\kappa B\alpha(t) + ki3a \times kv \times I\kappa B\alpha(t) - ke3a \times kv \times nI\kappa B\alpha(t) \quad \text{(A7)}$$

$$\frac{d}{dt} A20(t) = c2 \times tA20(t) - c4 \times A20(t) \quad \text{(A8)}$$

$$\frac{d}{dt} tI\kappa B\alpha(t) = c1a \times \frac{nNF\kappa B^h(t)}{nNF\kappa B^h(t) + k^h} - c3a \times tI\kappa B\alpha(t) \quad \text{(A9)}$$

$$\frac{d}{dt} tA20(t) = c1 \times \frac{nNF\kappa B^h(t)}{nNF\kappa B^h(t) + k^h} - c_3 \times tA20(t) \quad \text{(A10)}$$

$$\frac{d}{dt} pI\kappa B\alpha(t) = kc1a \times IKKa(t) \times I\kappa B\alpha(t) - kt1a \times pI\kappa B\alpha(t) \quad \text{(A11)}$$

$$\frac{d}{dt} (pI\kappa B\alpha \circ NF\kappa B)(t) = kc2a \times IKKa(t) \times (I\kappa B\alpha \circ NF\kappa B)(t) - kt2a \times (pI\kappa B\alpha \circ NF\kappa B)(t) \quad \text{(A12)}$$

$$\frac{d}{dt} (I\kappa B\alpha \circ NF\kappa B)(t) = ka1a \times I\kappa B\alpha(t) \times NF\kappa B(t) - kd1a \times (I\kappa B\alpha \circ NF\kappa B)(t) - c5a \times (I\kappa B\alpha \circ NF\kappa B)(t) + ke2a \times (nI\kappa B\alpha \circ nNF\kappa B)(t) - kc2a \times IKKa(t) \times (I\kappa B\alpha \circ NF\kappa B)(t) \quad \text{(A13)}$$

$$\frac{d}{dt} (nI\kappa B\alpha \circ nNF\kappa B)(t) = ka1an \times nI\kappa B\alpha(t) \times nNF\kappa B(t) - kd1a \times (nI\kappa B\alpha \circ nNF\kappa B)(t) - ke2a \times kv \times (nI\kappa B\alpha \circ nNF\kappa B)(t) \quad \text{(A14)}$$

B

Reaction	Symbol	Value	References
C:N ratio	*kv*	3.3	(Ashall et al., 2009)
Initial concentration			
Total NF-κB	-	0.08 μM	(Ashall et al., 2009)
Total IKK	-	0.08 μM	(Ashall et al., 2009)
IKK			
IKKn → IKKa	*ka*	0.004s^{-1}	(Ashall et al., 2009)
IKKa → IKKi	*ki*	0.003 s^{-1}	(Ashall et al., 2009)

IKKi → IKKn	*kp*	0.0006 s^{-1}	(Ashall et al., 2009)
A20 inhibition rate constant	***kbA20***	**0.0017**	**Fitted**
Complex formation & dissociation			
IκBα + NF-κB → IκBα·NF-κB nIκBα + nNF-κB → nIκBα·NF-κB	*ka1a*	0.5 $\mu M^{-1}s^{-1}$	(Ashall et al., 2009)
IκBα·NF-κB → IκBα + NF-κB nIκBα·nNF-κB → nIκBα + nNF-κB	*kd1a*	0.0005 s^{-1}	(Ashall et al., 2009)
A20 protein synthesis & degradation			
nNF-κB → nNF-κB + tA20 *Order of hill function, h=2* *Half-max constant, k=0.065*	*c1*	1.4×10^{-7} $\mu M^{-1}s^{-1}$	(Ashall et al., 2009)
tA20→ tA20 + A20	*c2*	0.5 s^{-1}	(Ashall et al., 2009)
tA20→ Sink	*c3*	0.00048 s^{-1}	(Ashall et al., 2009)
A20 → Sink	*c4*	0.0045 s^{-1}	(Ashall et al., 2009)
IκBα protein synthesis & degradation			
nNF-κB → nNF-κB + tIκBα *Order of hill function, h=2* *Half-max constant, k=0.065*	*c1a*	1.4×10^{-7} $\mu M^{-1}s^{-1}$	(Ashall et al., 2009)
tIκBα→ tIκBα + IκBα	*c2a*	0.5 s^{-1}	(Ashall et al., 2009)
tIκBα→ Sink	*c3a*	0.0003 s^{-1}	(Ashall et al., 2009)
IκBα→ Sink	*c4a*	0.0005 s^{-1}	(Ashall et al., 2009)
NF-κB·IκBα→ NF-κB	*c5a*	0.000022 s^{-1}	(Ashall et al., 2009)
IκBα & IKK interaction			
IκBα & IKK interaction			
IKKa + IκBα → pIκBα	*kc1a*	0.074 s^{-1}	(Ashall et al., 2009)
IKKa + IκBα·NF-κB → pIκBα·NF-κB	*kc2a*	0.185 s^{-1}	(Ashall et al., 2009)
pIκBα → Sink	*kt1a*	0.1 s^{-1}	(Ashall et al., 2009)
pIκBα·NF-κB → Sink	*kt2a*	0.1 s^{-1}	(Ashall et al., 2009)
Transport			
NF-κB → nNF-κB	*ki1*	0.0026 s^{-1}	(Ashall et al., 2009)
nNF-κB → NF-κB	*ke1*	0.00052 s^{-1}	(Ashall et al., 2009)
nIκBα·nNF-κB → IκBα·NF-κB	*ke2a*	0.01 s^{-1}	(Ashall et al., 2009)
IκBα → nIκBα	*ki3a*	0.00067 s^{-1}	(Ashall et al., 2009)
nIκBα → IκBα	*ke3a*	0.000335 s^{-1}	(Ashall et al., 2009)

C

Model equations		
Pathway activation	$Z(t+\delta t) = Z(t)(1-\rho)\delta t + D$	(C1)
Effective TNFα dose	$D \sim \min(D^*,1), \quad D \in (0,1]$ where $D^* \sim Pareto_{(\xi,\mu,\sigma)}(x) = \frac{\sigma^{\frac{1}{\xi}}}{\left(\sigma+\xi\left(x-\mu\right)\right)^{1+\frac{1}{\xi}}}$ for $x \geq \mu$ (Fig.8) Or $D^* \sim Exponential_{(\lambda)}(x) = \lambda e^{-\lambda \cdot x}$ for $x \geq 0$ (Fig. 7C)	

Receptor-IKK interaction	$\frac{d}{dt} IKKn(t) = kp \times \frac{kbA20}{kbA20+A20(t)} \times IKKi(t) - Z(t) \times ka \times IKKn(t)$ $\frac{d}{dt} IKKa(t) = Z(t) \times ka \times IKKn(t) - ki \times IKKa(t)$ $\frac{d}{dt} IKKi(t) = ki \times IKKa(t) - kp \times \frac{kbA20}{kbA20+A20(t)} \times IKKi(t)$	(C2) (C3) (C4)
Other reactions	As in Table S2A (Eq.(A4)-(A14))	(C5-C15)

Model parameters

Parameter	Symbol	Value	References
Z inactivation rate	ρ	$0.07s^{-1}$	Fitted
Simulation step size	δt	1s	Fitted
Pareto parameters	(ξ, μ, σ)	$(2,0,10^{-9})$	Simulations in Fig. 8A
Pareto parameters (alternative set)	(ξ, μ, σ)	$(1.8,0,10^{-6})$	Simulations in Fig. 8B
Exponential parameters	λ	3×10^{5}	Simulations in Fig, 7C
Other parameters	As in Table S2B		